An Agent-Based Model of Plant Disease Diffusion and Control:

Grapevine Leafroll Disease

Shady S. Atallah[1], Miguel I. Gómez[2], Jon M. Conrad[3], and Jan P. Nyrop[4]

[1] PhD student, sa589@cornell.edu
[2] Assistant Professor, mig7@cornell.edu
[3] Professor, jmc16@cornell.edu
[4] Professor, jpn2@cornell.edu

Dyson School of Applied Economics and Management
Cornell University

Selected Paper prepared for presentation at the Agricultural & Applied Economics Association's 2012 AAEA Annual Meeting -Seattle, August 12-14

An Agent-Based Model of Plant Disease Diffusion and Control: Grapevine Leafroll Disease

Abstract: The grapevine leafroll disease (GLRD) threatens grape harvests in the United States and the world. This viral disease reduces yield, delays fruit ripening, and affects wine quality. The disease ecology is still under study and the spatial-dynamics of the spread process remains poorly understood. Moreover, little is known about cost-efficient strategies to control the disease. In an effort to address this gap in the literature, we model GLRD diffusion in a vineyard and evaluate bioeconomic outcomes under alternative disease control strategies. We employ agent-based modeling (ABM) tools and contribute to the bioeconomic literature on agricultural disease control in several ways. First, our model relaxes the assumption of agent homogeneity and allows instead agents to be heterogeneous in age and infection states, thus in their economic values. Second, we make the model inherently spatial-dynamic by combining the ABM with a cellular automaton system. Third, we incorporate realism when modeling the spread process by making the disease onset and its transmission stochastic. That is, initial infections follow a random spatial distribution and stochastic agent interaction gives rise to Markov process-type disease diffusion. Finally, we formulate novel control strategies consisting of roguing and replacing infected grapevines based on their age and infection states. We evaluate these strategies and identify those that perform best at extending the expected vineyard half-life and at maximizing the vineyard expected net present values relative to the baseline of no control. The model results underscore the ecological and economic tradeoffs implied by disease control strategies based on age and infection states.

Key words: grapevine leafroll disease, bioeconomic models, agent-based model, spatial-dynamic process, disease control

The grapevine leafroll disease (GLRD) presently threatens grape harvests in the United States (Fuchs et al. 2009, Golino et al. 2008, Martin et al. 2005) and the world (Cabaleiro et al. 2008, Charles et al. 2009, Freeborough and Burger 2008, Martelli and Boudon-Padieu 2006). This viral disease reduces yield, delays fruit ripening, and affects wine quality by lowering soluble solids and increasing fruit juice acidity (Goheen and Cook 1959, Martelli and Boudon-Padieu 2006, Martinson et al. 2008). Its economic impact was recently estimated at $25,000- $40,000 per hectare over a 25 year-period in New York State vineyards if the disease if left uncontrolled (Atallah et al. 2012). GLRD is primarily transmitted via vegetative propagation and grafting. There is increasing evidence however that, once the disease is introduced through infected planting material, it is spread and transmitted to healthy vines by several species of mealybugs (Hemiptera: Pseudococcidae) and soft-scale insects (Hemiptera: Coccidae) (Martelli and Boudon-Padieu 2006, Pietersen 2006, Tsai et al. 2010). Recent plant pathology studies have examined the spatiotemporal insect-facilitated diffusion patterns of the disease (Cabaleiro et al. 2008, Jooste et al. 2011). However, the disease ecology is still under study and the spatial-dynamics of the spread process remains poorly understood. Moreover, we know very little about cost-efficient strategies to control the disease diffusion.

Multiple disciplines have taken complementary approaches when modeling disease diffusion and control, including ecology, economics and epidemiology, among others. Generally, this literature employs state equation-based methods (often referred to as top-down methods) with simplifying assumptions in order to achieve mathematical rigor. However, such methods are not suitable for characterizing the spatial-dynamic processes underlying diffusion processes (Wilen 2007) or the agents under study (Miller and Page 2007). Assumptions made in these top-down models such as agent homogeneity are too restrictive, particularly for policy-makers who might

want to target disease intervention programs to specific agents based on their role in disease transmission (Greenhalgh 2010). More recently, with dramatic decreases in computational costs, agent-based modeling (ABM) has gained popularity as a new theoretical framework to study complex adaptive systems (Miller and Page 2007). Disease diffusion systems can be treated as complex adaptive systems (CAS) because they are composed of adaptive agents whose interaction produces outcomes that cannot be wholly explained by breaking down the system into its individual parts (Miller and Page 2007, Teose et al 2011).The bottom-up approach of ABM allows sophisticated interactions between agents with heterogeneous state space. However, their primary disadvantage is that the relatively easier model construction and validation of top-down equation-based models is lost (Osgood 2007). ABMs are also harder to parameterize and validate (Rahmandad and Sterman 2008). When used in epidemiological research, these two modeling paradigms have yielded results that are consistent at times (e.g. Schneckenreither et al 2008) and divergent in their public policy implications in other cases (e.g. Rahmandad and Sterman 2008).

This paper develops an agent-based computational economic model of disease diffusion and control. The model allows for a full spatial-dynamic characterization of the disease diffusion, relaxing the assumptions of homogeneity and perfect mixing. Instead, disease control takes into account agent heterogeneity in age and infection stage. We examine the impact of disease control strategies on a distribution of bioeconomic outcomes and rank them based on their cost-effectiveness. Our results highlight the ecological and economic tradeoffs involved in the timing of disease control in a population that is heterogeneous in age and infection stage. The simulations results provide vineyard managers information to identify novel and cost-effective strategies for GLRD control. Our results can be generalized to viral disease diffusion and control in other managed plant systems such as fruit orchards. We are not aware of previous work in the

agricultural and resource economics literature that applies agent-based simulation tools to model and study agricultural disease diffusion and control.

This paper is organized as follows. In the second part, we review the literature on insect-transmitted viral diseases and the economic literature on agricultural disease control. Those literatures inform our choice of conceptual framework which we describe in the third part. We then interpret and discuss the simulation results of the disease diffusion and control, conclude with insights and suggest areas for future research.

A. Related literature

Diffusion and control of insect-transmitted viral diseases such as GLRD have characteristics that are supported by certain modeling approaches and not others. First, the insect vector density needed for rapid disease spread is low (Holt and Chancellor 1996). This is particularly true for mealybugs and soft-scale insects in vineyards, rendering vector control methods ineffective (Cabaleiro and Segura 2006). Instead, disease control relies on measures aimed at minimizing secondary sources of virus infection by roguing (removing) infected plants and replacing them with healthy ones (Chan and Jeger 1994). Second, in viral disease, the relationship between pest populations and crop yield or quality is complex, contrary to cases in which pest-population density is the main parameter used in damage assessment (Bos 1982). These two unique characteristics of viral diseases limit the applicability of existent pest control and damage control models (e.g., Babcock et al 1992, Saphores 2000). Third, virus diseases have an initial latent period during which plants are not infectious (Chan and Jeger 1994). Moreover, for certain viral diseases, including GLRD, the latency period seems to be age-dependent as older plants tend to have longer latency periods (Pietersen 2004). This implies the need for models structured by age

and infection states but also the opportunity to explore novel disease management strategies that take those states into account. The bioeconomic and resource economics literatures offer models that are structured by infection (e.g. Horan et al. 2010) or age (e.g. Tahvonen 2010) stages, but few are structured by both states[1] and the literature is mostly non-spatial (Wilen 2007). That brings us to the last but not least characteristic of viral diseases; they are driven by integrated dynamic and spatial forces, rather than by dynamics processes alone.

Spatial-dynamic processes have only recently been studied by economists (e.g. Sanchirico and Wilen 1999, 2005; Epanchin-Niell and Wilen 2012); tools are available to study them, although the most realistic ones preclude analytical solutions and require numerical methods (Wilen 2007). We will briefly review the economic literature on agricultural disease control and the agent-based computational modeling literature in order to be able to relate later how we borrow the tools of the latter in order to study the problems of the former.

The economic literature on agricultural disease control has increasingly moved away from pest threshold models (Hall and Norgaard 1973). Instead, it has integrated equation-based epidemiological models (Beach et al. 2007, Fenichel and Horan, 2007, Horan and Wolf, 2005) to incorporate feedbacks between the economic and disease spread model components so that ecological thresholds and economic trade-offs are simultaneously determined. Traditionally, population disease state transition has been modeled using ordinary differential equations (ODEs) and optimal disease control strategies have been solved for using linear and non-linear programming, optimal control and/or dynamic optimization methods (e.g., Bicknell et al 1999).

[1] Greenhalgh (2010) surveys age-structured epidemic models (i.e. structured by both age and infection states) aimed at disease eradication. Horan et al. (2010) review ecological models that impose disease eradication as a goal *a priori* and discuss the limitations of such models that treat disease management as exogenous to the system.

However, ODEs are limited in their ability to explicitly model the spatial dimension of disease diffusion. For this reason, partial differential equations (PDEs) are preferred as they allow more realism through the simultaneous incorporation of the temporal and spatial processes (Holmes et al 1994). However, most PDEs are either difficult or impossible to solve analytically, leading to either the use of very simple models or the development of complex numerical models (Wilen 2007). Another limitation of top-down equation-based disease models using ODEs or PDEs is their underlying assumption that populations are homogeneous (Brauer and Castillo-Chavez, 2001). This assumption is unrealistic in epidemiology where population age-structure is a critical factor influencing disease spread (Greenhalgh 2010). The population homogeneity assumption is particularly restrictive when innovative disease control strategies are sought to control the disease diffusion (e.g. Hadeler and Muller 1996).

In contrast to equation-based modeling, agent-based models[2] (ABMs) allow the study of a population of heterogeneous agents living in a spatial structure with a rich state space. They are computationally intensive dynamic simulation models where agents are given states and simple rules and then left to interact with their environment and each other according to those rules (Tesfatsion 2006). Agent interaction gives rise to a distribution of system-wide non-linear outcomes that are of interest to the researcher and that cannot usually be deduced from the simple rules given to the agents. They are appropriate in high-resolution models because they represent spatial actors with relatively complex properties in a straightforward way; they are computationally efficient; and they capture the interactive properties of natural and human systems as well as the complex outcomes that emerge from this interaction (White and Engelen 2000).

[2] Also called Agent-based Computational Economics (ACE) models in economics (Tesfatsion 2006) and Individual-based Models (IBMs) in ecology (Railsback and Grimm 2012)

They are appealing because they offer a good trade-off between flexibility (ability to capture a wide class of behaviors) and precision (exact definition of model elements); they are inherently dynamic, scalable (number of agents), fully observable and repeatable (table 1).

The agent-based computational economics literature has explored feedbacks between social and ecological systems with applications in ecological economics (e.g. Jager et al 2000), microeconomic policy (e.g. Chen and Chie 2008), industrial organization (e.g. Barr and Saraceno 2005), and technological change (Nelson and Wright 1992) among others. ABM can be used to simulate the spatial-dynamic diffusion of an agricultural disease in a heterogeneous population and can yield distributions of bioeconomic outcomes under different disease control. This is particularly relevant and applicable to the spread of the grapevine leafroll disease in a vineyard where vines are heterogeneous in their static (location) and dynamic attributes (age and infection stages).

We contribute to the disease control bioeconomic literature by applying the tools of agent-based modeling to an agricultural disease spread and control problem. By integrating cellular automata with agent-based systems, we offer a model that is inherently spatial-dynamic. We allow agents to be heterogeneous with static and dynamic attributes. Disease is initialized following a random spatial distribution and stochastic agent interaction gives rise to disease diffusion. Distributions of bioeconomic outcomes are generated and evaluated for the baseline case of no control and under alternative disease control strategies.

B. Conceptual framework

We develop a stochastic agent-based model of disease diffusion and control that is discrete in both time and space. The model is spatially explicit and the population consists of agents that are

heterogeneous in their location, age and infection stages. In this section we define the agents, their environment, their interactions and the state transitions.

1. Agents

In this model, an agent represents a grapevine and the grid on which agents live represents a vineyard. A typical agent is characterized by its *attributes* (static and dynamic) and the *methods* that give agents the ability to perceive their environment, including agents in their vicinity and the ability to perform actions such as sending messages to other agents (Macal and North, 2010). An agent's memory records its previous state and action (Gilbert 2008). Each agent in this model is endowed with one *static* state, namely its location on the grid. Agents also have three *dynamic* states: age, own infection state, and the neighbors' infection state. The location static state is used to make the disease spatial spread limited by the vineyard boundaries and geometry. The dynamic age and infection states are used to model the age-dependence of the latency period (the time before an infected vine becomes infective) and agent heterogeneity in infection and age states that translate into heterogeneity in the agents' economic values.

Agents' *methods* are rules governing how an infectious agent perceives the location and infection status of neighboring vines and transmits the disease to within-row neighbors with a higher probability than it does to neighbors in the adjacent row. This is needed for transition rules to mimic spatial patterns of disease diffusion observed in spatial analyses of GLRD (Habili et al. 2008; Cabaleiro et al. 2008). Those rules govern disease diffusion and are therefore crucial when evaluating the impacts of disease control policies.

2. Agent environment: cellular automaton

Agents are often modeled as operating within an environment consisting of a network of interactions with other agents. Specifically, when the physical environment includes constraints on

the agent's spatial environment, such as boundaries and geometry, agent-based models should be combined with cellular automata systems (Gilbert and Terna, 2000).

Cellular automata (CA) are discrete dynamical systems that operate in space and time on a uniform and regular lattice of cells. They model complex behavior based on simple, local state transition rules animating the cells. At each time step, each cell computes its new state given its old state and the states of its closest neighbors according to the transition rules (Tesfatsion 2006, Wolfram 1986). CA are attractive, especially when used with ABMs because they provide agents with a rule-based, spatial-dynamic structure; they are adaptable and can thus represent a variety of processes; they are simple, thus computationally efficient and yet exhibit rich behavior (White and Engelen 2000). Using a cellular automaton system in an agent-based model provides an adequate spatiotemporal simulation environment for the diffusion of the grapevine leafroll disease and the evaluation of alternative disease control strategies: the vineyard is represented by a grid where cells are occupied by agents (i.e. the vines) whose infection and age states, locations and interactions determine GLRD spread. In what follows, we describe the five elements of the cellular automaton and the features they convey the agent-based model that integrates them. Those are the cell, the cell states, the cell neighborhood, the cell transition rules and the time step.

a) The cells

Cells are the units that make up the two-dimensional grid. The grid represents a vineyard plot with (I x J) cells where I and J are the number of rows and columns, respectively. In our model, there are 5,720 cells each holding only one agent representing a grapevine. Vineyard rows are oriented north to south with I=44 vines per row and J=130 vines per column. This configuration is

considered representative of a typical Northeastern vineyard in the US[3,4] (Wolf 2008). Each cell can hold only one state at any point in time. Next, we define the cell state space.

b) The cell states $W_{i,j}^{t}$

The state of a cell located in row *i* and column *j* at time *t+1* ($W_{i,j}^{t+1}$) can be represented as a function *f* of the cellular automaton's elements at time *t* as follows (Ozah et al 2010):

$$W_{i,j}^{t+1} = f(W_{i,j}^{t}, N_{i,j}^{t}, R_{i,j}, \Delta t) \quad (1)$$

where $W_{i,j}^{t}$ is the state of a cell (i ,j) in time t ; $N_{i,j}^{t}$ is the neighborhood (made up of neighboring cells) of cell (i ,j) at time t; $R_{i,j}$ is the state transition rule; and Δt the time step. $W_{i,j}^{t}$ is an age-infection composite state defined as the combination of a vine's age state $A_{i,j}^{t}$ and a vine's infection $S_{i,j}^{t}$. The infection state space $S_{i,j}^{t}$ of a vine located at cell (i, j) is {H, E, I_m, I_h}. H is the *Healthy* state that describes vines that are susceptible to infection. E is the *Exposed* or latent infection state, during which a vine is infected, symptomless, and not yet infective. I_m (*Infective-moderate*) and I_h (*Infective-high*) represent the states of infective grapevines with moderate and high disease severity, respectively. [5] When describing the location-dependent disease transmission, we will refer to states H and E collectively as the composite state *NI* (*Non-infective*) in which a vine in non-infective. Similarly, we will refer to states I_m and I_h collectively as the composite state *I* (*Infective*) that denotes vines that have the ability to transmit the infection.

[3] The represented vineyard dimensions would then be 350' x 650'with an area of 227,500 ft^2 or 5.22 acres.

[4] We choose a vineyard configuration that is representative of this region because we previously assessed the economic impact of GLRD in New York State vineyards (Gómez et al 2010; Atallah et al 2012).

[5] Harper et al (1975) define the potato leafroll disease severity through the extent of foliage symptoms severity: none, mild, slight, moderate and severe symptoms.

The age state space of a vine $A_{i,j}^{t}$ is $\{1, 2, \ldots, A_{max}\}$. Combining the infection states and the age states into a space of composite age-infection states $W_{i,j}^{t}$ allows modeling the fact that (1) younger vines have shorter latency periods (Pietersen 2006), i.e. they transition from *E* to I_m faster than older vines; and (2) a vine's economic value increases with the age state transition but decreases with the infection state transition[6]. When modeling the age-dependent latency transition, we discretize the age space into *Young* (0 to 5 years), *Mature* (5-20 years) and *Old* (20 years and above) age categories based on vines' age-specific state transition rates.

c) The cell neighborhood $N_{i,j}^{t}$ and its state $S_{N_{i,j,k}}^{t}$

Charles et al (2009) observed that once GLRD is introduced through unsanitary vines at planting in a random spatial pattern, leafroll-associated viruses are transmitted through vectors (mealybugs) with limited mobility within rows through dispersal of infected mealybug crawlers. The virus is transmitted to a lesser extent across rows either through human-assisted movement of mealybug crawlers or through aerial dispersal of infective mealybugs (resulting in random infections of vines) (Cabaleiro et al. 2008, Jooste et al. 2011).

Given the limited mobility of the grapevine leafroll disease vectors, we give the agents a von Neumann neighborhood type[7] in which each agent has four neighbors in the four cardinal directions (north, south, east, west) (figure 1). This neighborhood type offers the capability of defining different transition rules (infection transmission rates) within vineyard rows (e.g. north

[6] As a vine goes through the four infection states, its economic value decreases as the grapevine yield and grape juice quality are reduced. The age state acts in the opposite direction: as a vine transitions within age states, its economic value increases.

[7] Two-dimensional cellular automata models can also have a Moore type neighborhood with eight neighboring cells in the cardinal and inter-cardinal directions.

and south) and across rows (e.g. east and west). This allows us to model the observed faster within-row spread of the disease (Habili et al 1995). For a vine $V_{i,j}$ located in cell (i, j), the neighborhood $N_{i,j}^t$ can be expressed as:

$$N_{i,j}^t = \{ V_{i,j-1}, V_{i,j+1}, V_{i-1,j}, V_{i+1,j} \} \quad (2)$$

$$(j-1) \in \{1, J-1\}; (j+1) \in \{1, J-1\}; (i-1) \in \{1, I-1\}; (i+1) \in \{2, I\}$$

where the first two elements represent adjacent-row neighbors to the west and to the east and the last two elements represent same-row neighbors to the north and south. The intervals on the indices of vine (i, j)'s neighbors define the boundaries of the vineyard.

[Figure 1 here]

The infectivity state of the neighborhood of a cell *(i,j)* at time *t*, denoted by $S_{N_{i,j,k}}^t$, is determined by the individual infectivity (*Infective* and *Non-infective*) states ($S_{i-1,j}^t$ $S_{i+1,j}^t$, $S_{i,j-1}^t$, $S_{i,j+1}^t$) of the four neighboring cells *(i-1, j), (i+1, j), (i,j-1), and (i, j+1)*. Given two possible infectivity states and four neighbors, $S_{N_{i,j,k}}^t$ can be one of 2^4 possible neighborhood infectivity states ($S_{i-1,j}^t$ $S_{i+1,j}^t$, $S_{i,j-1}^t$, $S_{i,j+1}^t$) enumerated in the set $S_{N_{i,j,k}}^t$ where $k \in \{1, 2, ..., 16\}$ and

$$S_{N_{i,j,k}}^t \in \{S_{N_{i,j,1}}^t = (I, I, I, I), S_{N_{i,j,2}}^t = (I, I, I, NI), S_{N_{i,j,3}}^t = (I, I, NI, I), S_{N_{i,j,4}}^t = (I, I, NI, NI), \quad (3)$$

$$S_{N_{i,j,5}}^t = (I, NI, I, I), S_{N_{i,j,6}}^t = (I, NI, I, NI), S_{N_{i,j,7}}^t = (I, NI, NI, I), S_{N_{i,j,8}}^t = (I, NI, NI, NI),$$

$$S_{N_{i,j,9}}^t = (NI, I, I, I), S_{N_{i,j,10}}^t = (NI, I, I, NI), S_{N_{i,j,11}}^t = (NI, I, NI, I), S_{N_{i,j,12}}^t = (NI, I, NI, NI),$$

$$S_{N_{i,j,13}}^t = (NI, NI, I, I), S_{N_{i,j,14}}^t = (NI, NI, I, NI), S_{N_{i,j,15}}^t = (NI, NI, NI, I), S_{N_{i,j,16}}^t = (NI, NI, NI, NI)\}$$

d) The cell transition rules

The cell transition rules control the transitions within each of the age state and the infection state spaces. Given that age transitions are deterministic, we focus on the stochastic infection state transitions affecting the spatiotemporal diffusion of the disease. We describe the stochastic

initialization of the model states, the stochastic location-dependent infection transitions from *Healthy* to *Exposed*[8]; the deterministic age-dependent infection transitions from *Exposed* to *Infective*; and the deterministic transition within the *Infective* state (I_m to I_h). We finally represent the infection transition rules in a Markov chain model.

Model Initial States

At the beginning of a simulation, 2 percent of the agents, homogeneous in their age-infection states ($S_{i,j}^t = H$ and $A_{i,j}^t = 0$), are chosen at random from a uniform distribution U (0, 5720) to transition from *Healthy* to *Exposed*. This reflects findings in leafroll spatial analyses indicating that primary infection sources are spatially randomly distributed (Cabaleiro et al. 2008), and that initial disease prevalence is typically between 1 and 5 percent (Atallah et al 2012). Thereafter, GLRD spreads to uninfected vines according to rules that govern state transitions from *Healthy* to *Exposed*, *Exposed* to *Infective* and *Infective-moderate* to *Infective-high states*.

Stochastic location-dependent Healthy (H) to Exposed (E) state transition

An infective vine transmits the virus to a neighboring healthy vine with a location-specific transmission rate. Following Cabaleiro et al. (2008), infective vines transmit the disease to their same-row neighbors at a higher rate than they transmit it to their adjacent-row neighbors. The continuous-time transmission rates are assumed to follow a Poisson process. That is, the waiting time X that it takes for a vine in the *Healthy* state to transition to the *Exposed* state is assumed to have an exponential distribution[9] with parameter α for same-row transmission ($X_1 \sim \alpha e^{-\alpha X_1}$) and β for adjacent-row transmission ($X_2 \sim \beta e^{-\beta X_2}$) with $0<\beta<\alpha$. Then, the probability that a vine transitions from a *Healthy* state in period t to an *Exposed* state in period t+1 is Pr ($X_1 <1$) = 1 - $e^{-\alpha}$ for same-row transmission and Pr ($X_2 <1$) = 1 - $e^{-\beta}$ for adjacent-row transmission.

[8] Recall that the *Exposed* state is one where a vine is infected, symptomless, and not yet infective

[9] This is a standard assumption in epidemic models (Greenhalgh 1986)

Let ***B*** be the *Healthy* to *Exposed* vector of transition probabilities conditional on previous own and neighborhood infection states. Mathematically, it can be expressed as

$$\boldsymbol{B} = \begin{pmatrix} \Pr(S_{i,j}^{t+1} = E \mid S_{i,j}^{t} = H,\ S_{N_{i,j,k}}^{t} = S_{N_{i,j,1}}^{t}) \\ \Pr(S_{i,j}^{t+1} = E \mid S_{i,j}^{t} = H,\ S_{N_{i,j,k}}^{t} = S_{N_{i,j,2}}^{t}) \\ \Pr(S_{i,j}^{t+1} = E \mid S_{i,j}^{t} = H,\ S_{N_{i,j,k}}^{t} = S_{N_{i,j,3}}^{t}) \\ \Pr(S_{i,j}^{t+1} = E \mid S_{i,j}^{t} = H,\ S_{N_{i,j,k}}^{t} = S_{N_{i,j,4}}^{t}) \\ \vdots \\ \Pr(S_{i,j}^{t+1} = E \mid S_{i,j}^{t} = H,\ S_{N_{i,j,k}}^{t} = S_{N_{i,j,13}}^{t}) \\ \Pr(S_{i,j}^{t+1} = E \mid S_{i,j}^{t} = H,\ S_{N_{i,j,k}}^{t} = S_{N_{i,j,14}}^{t}) \\ \Pr(S_{i,j}^{t+1} = E \mid S_{i,j}^{t} = H,\ S_{N_{i,j,k}}^{t} = S_{N_{i,j,15}}^{t}) \\ \Pr(S_{i,j}^{t+1} = E \mid S_{i,j}^{t} = H,\ S_{N_{i,j,k}}^{t} = S_{N_{i,j,16}}^{t}) \end{pmatrix} = \begin{pmatrix} 1 - e^{-(2\alpha+2\beta)} \\ 1 - e^{-(2\alpha+\beta)} \\ 1 - e^{-(2\alpha+\beta)} \\ 1 - e^{-2\alpha} \\ 1 - e^{-(\alpha+2\beta)} \\ 1 - e^{-(\alpha+\beta)} \\ 1 - e^{-(\alpha+\beta)} \\ 1 - e^{-\alpha} \\ 1 - e^{-(\alpha+2\beta)} \\ 1 - e^{-(\alpha+\beta)} \\ 1 - e^{-(\alpha+\beta)} \\ 1 - e^{-\alpha} \\ 1 - e^{-2\beta} \\ 1 - e^{-\beta} \\ 1 - e^{-\beta} \\ 0 \end{pmatrix} \quad (4)$$

where there are 2^4 possible neighborhood infectivity states, but only nine distinct conditional probabilities. This is because an infective agent to the north of a healthy agent transmits the disease with the same probability as the neighbor to the south does. Similarly, an infective agent to the east transmits the disease with the same probability as the neighbor to the west does.

The *Healthy* to *Exposed* state transition probabilities are governed in each time step by a random variable u_t. Where u_t is a random draw from $U\sim(0,1)$, the disease is transmitted from one infective vine to another healthy vine in the same row at time $t+1$ if $u_t \geq \alpha$. Conversely, the disease is not transmitted if $u_t<\alpha$. Similarly, the disease is transmitted from one infective vine to another healthy vine in the adjacent row at time $t+1$ if $u_t \geq \beta$ and is not transmitted if $u_t < \beta$.

Deterministic age-dependent Exposed (E) to Infective (I) state transition

In order to account for shorter latency periods in younger vines, we age-structure the vine population as follows: *Young* (0 to 5 years), *Mature* (5 to 20 years) and *Old* (above 20 years); and

assume that the latency periods for young (L_y), mature (L_m) and old (L_o) vines follow exponential distributions with fixed rate parameters $\lambda_y, \lambda_m, \lambda_o$: $L_y \sim \text{Exp}(\lambda_y)$, $L_m \sim \text{Exp}(\lambda_m)$, $L_o \sim \text{Exp}(\lambda_o)$ where $\lambda_y < \lambda_m < \lambda_o$. The probability that a vine transitions from *Exposed* to *Infective* in one time step is defined for young, mature and old vines respectively as follows: $\Pr(L_y < 1) = 1 - e^{-\lambda_y}$, $\Pr(L_m < 1) = 1 - e^{-\lambda_m}$, $\Pr(L_o < 1) = 1 - e^{-\lambda_o}$. The *Exposed* to *Infective* state transition probabilities conditional on age category can be represented mathematically in the vector $\boldsymbol{C}$ where:

$$\boldsymbol{C} = \begin{pmatrix} \Pr\left(S_{i,j}^{t+1} = I \,\middle|\, S_{i,j}^{t} = E,\ A_{i,j}^{t} = Young\right) \\ \Pr\left(S_{i,j}^{t+1} = I \,\middle|\, S_{i,j}^{t} = E,\ A_{i,j}^{t} = Mature\right) \\ \Pr\left(S_{i,j}^{t+1} = I \,\middle|\, S_{i,j}^{t} = E,\ A_{i,j}^{t} = Old\right) \end{pmatrix} = \begin{pmatrix} 1 - e^{-\lambda_y} \\ 1 - e^{-\lambda_m} \\ 1 - e^{-\lambda_o} \end{pmatrix} \quad (5)$$

Deterministic transition from Infective-moderate (I_m) *to* Infective-high (I_h)

Once a vine is infected at the moderate level, symptoms worsen over time and reach a high level after a fixed amount of time, denoted by *Inf*. The period that a vine spends in state I_m before it transitions to state I_h is assumed to be exponentially distributed with fixed rate parameter φ: $Inf \sim \text{Exp}(\varphi)$. Thus, the probability that a vine transitions from I_m to I_h in one time step is defined as $\Pr(Inf < 1) = 1 - e^{-\varphi}$ or $\Pr\left(S_{i,j}^{t+1} = I_h \,\middle|\, S_{i,j}^{t} = I_m\right) = 1 - e^{-\varphi}$.

Markov Chain Model

Agent state transitions are governed by a Markov chain model defined by a set of states and a set of transitions with associated conditional probabilities defining a distribution over the next possible states. Specifically, the model is a homogenous Markov chain assuming that the transition probabilities are unique, depend only on the current state and not on state history, and are time invariant. A homogenous Markov chain modeling agent state transition can be represented by

$$\boldsymbol{S_{i,j}^{t+1}} = \boldsymbol{P}\ \boldsymbol{S_{i,j}^{t}} \quad (6)$$

where $\boldsymbol{S_{i,j}^t}$ is the agent's infection state vector at time *t* of dimension 4 x1. The vector holds a 1 for the state that describes the agent's infection status and zeros for the remaining 3 states,

and

$$\boldsymbol{P} = \begin{pmatrix} (\mathbf{1}-\boldsymbol{B})^T & \boldsymbol{B}^T & 0 & 0 \\ 0 & (\mathbf{1}-\boldsymbol{C})^T & \boldsymbol{C}^T & 0 \\ 0 & 0 & e^{-\varphi} & (1-e^{-\varphi}) \\ 0 & 0 & 0 & 1 \end{pmatrix} \quad (7)$$

where vector $\boldsymbol{B}$ returns the *H* to *E* transition probability conditional on the agent's neighborhood infection state and vector $\boldsymbol{C}$ returns the *E* to I_m transition probability conditional on the agent's age state. The transition probability matrix $\boldsymbol{P}$ is read from row (states *H*, *E*, I_m, I_h at time *t*) to column (states *H*, *E*, I_m, I_h at time *t*+1). The infection state of cell (*i*, *j*) after *n* time steps is given by

$$\boldsymbol{S_{i,j}^n} = \boldsymbol{P^n}\, \boldsymbol{S_{i,j}^0} \quad (8)$$

where $\boldsymbol{S_{i,j}^0}$ is the agent's initial 4 x 1 infection state vector. Given that age is deterministic, the composite infection-age state of cell (*i*, *j*) after *n* time steps is similarly given by

$$\boldsymbol{W_{i,j}^n} = \boldsymbol{P^n}\, \boldsymbol{W_{i,j}^0} \quad (9)$$

where $\boldsymbol{W_{i,j}^0}$ is the agent's initial 4 x 1 infection-age state vector.

e) The time step

Time is modeled in discrete time steps. The simulation starts at time step zero, representing the vineyard establishment and proceeds until year 50. The cell states are updated after discrete time steps for all cells. We choose a month to be the time step; this is probably the most appropriate time step for a vineyard manager making disease control decisions. We calibrate the time dependent model parameters in a way that makes our baseline disease-spread simulation fall within ranges of disease spread curves reported in the GLRD literature (Cabaleiro et al. 2008, Cabaleiro

and Segura 2006). We choose parameter values from ranges reported in the literature and by consulting experts (table 1).

[Table 1 here]

3. Economic model

Disease diffusion outcomes are mapped into economic outcomes through the damages associated with the disease and the costs incurred when disease control policies are implemented. We layout in this section the economic model used to map the disease diffusion outcomes into economic outcomes.The revenue from a vine located in cell (*i*,*j*) that has composite age-infection state $W_{i,j}^{t}$ at time *t* depends on its infection status and age. A vine is unproductive at initial planting or replanting and it reaches its full yield potential after τ_{max} periods. When a grapevine is infected, its yield declines as does the price paid for its grapes due to quality losses.

a) Disease damage and control

A vineyard manager deciding whether to rogue and replace infected vines considers the cost of disease control relative to disease damage. Disease control costs are: (1) the costs of labor, machinery and material involved in roguing and replacing vines; (2) the opportunity cost of this control measure caused by the forgone revenues between the time control takes place and the time a newly planted vine bears fruit. Disease damages are: (1) the reduction in revenues of uncontrolled infected vines ($r_{w_{i,j,t}}$); (2) the expected losses that those vines will generate by spreading the infection to uninfected vines.

Vine-level disease damage is modeled through a reduction in the per-vine revenue $r_{w_{i,j},t}$ that depends on the composite age-infection ($w_{i,j,t}$) of a vine located at cell (i, j) at time *t*. We choose revenue values (table 2) that build on GLRD literature and interviews with vineyard managers in New York State (Gómez et al 2010, Atallah et al. 2012). For the infection states of

Susceptible, *Exposed*, *Infected-moderate* and *Infected-high*, yield reductions are 0, 30, 50, and 75 percent, respectively. Quality reduction is reflected in a 10 percent reduction in price paid for grapes, regardless of the infection state. Once a grapevine is infected, it transitions through the infection states and remains infected unless rogued and replaced. If rogued and replaced, the age-infection state of a vine is reset to its initial values ($S_{i,j}^{t} = H$ and $A_{i,j}^{t}$=0). Roguing and replacing a grapevine involves a per unit cost $c_{i,j}$. The vineyard-level revenues at each point in time are the sum of the revenues from each individual grapevine.

[Table 2 here]

b) Expected net present value of disease damage and control

Among a set of disease control strategies, a vineyard manager chooses the one that maximizes the vineyard expected net present value[10] across space and time:

$$\sum_{t\in T, t\geq 0} \rho^{t} * \{ \sum_{(i,j)\in C} \sum_{w_{i,j}\in S} [r_{w_{i,j},t} * (1 - \sum_{\tau=0}^{\tau_{max}} u_{w_{i,j},t-\tau}) - \sum_{\tau=0}^{\tau_{max}} (u_{w_{i,j},t-\tau} * c_{i,j})]\} \quad (10)$$

subject to (9), and:

$$r_{w_{i,j},0} = 0 \quad \text{for all } (i,j) \quad (11)$$

$$u_{w_{i,j},0} = 0 \quad \text{for all } (i,j) \quad (12)$$

where

ρ^{t} is the discount factor at time t (t>0), where $\rho^{t} = 1/(1+r)^{t}$ and r is the discount rate[11]

$t \in T$ indexes time, where $T=\{0,1,2,\ldots,T_{max}\}$

$\tau \in \{1,2\ldots, \tau_{max}\}$ where τ_{max} is the amount of time it takes a newly planted vine to become productive;

[10] We do not include costs other than disease control costs because they are unchanged under the different disease control strategies
[11] The discount rate is scaled to match the time step (see Table 2).

$(i,j) \in C$ indexes cells in row i and column j of the cellular automata grid, and C is the set of all cells in the grid;

$u_{w_{i,j},t} \in \{0, 1\}$ is a binary-choice variable equal to one if infected vine in cell (i,j) and state $W_{i,j}$ is rogued (removed) and replaced at time t and zero otherwise ;

$r_{w_{i,j},t} \in R_{w_{i,j},t}$ is the revenue of a vine in cell (i, j) that has age-infection state $W_{i,j}$ at time t; $R_{w_{i,j},t}$ is the space of possible revenues for all states;

$c_{i,j}$ is the cost of removing a vine from cell (i, j) and replacing it with a healthy vine

If a vine in state $w_{i,j,t}$ is rogued and replaced at time τ, then $u_{w_{i,j,t-\tau}}$=1 and the first term in the squared brackets equals zero (i.e. vines that have been planted in the previous τ time units are still unproductive), and the second term takes the value of the roguing and replacement cost.

If a vine in state $w_{i,j,t}$ is not rogued and replaced at time τ, then $u_{w_{i,j,t-\tau}}$=0 for all τ between 0 and τ_{max}, and the first term in the squared brackets takes the value of a vine's revenue, which depends on its age-infection state, and the second term equals zero.

C. Experimental Design

We evaluate disease control strategies that are based on the agent age and infection states. Combining age and infection states is important for two reasons. On the disease diffusion side of the model, age determines how fast vines become infectious and thus affect the disease spread. On the disease control side of the model, the age-infection state combination determines the economic value of the heterogeneous vines; a vine's value increases with age and decreased as it transitions through the infection states until it reaches the final absorbing composite state *Infected-high and Old* (I_hO).

Simulation experiments

Each experiment consists of a set of 1,000 simulation runs on a vineyard of 5,720 grapevines. Experiments differ in the age-infection disease control strategies they employ. Within an experiment, outcome realizations in each run differ due to the random spatial initialization (randomly selected locations of initial infections) and the random spatial disease diffusion. Data collected over simulation runs are the probability density functions of two outcomes under each strategy. Below, we describe the disease control strategies that differ under each experiment and the bioeconomic outcomes measured.

1. Disease control strategies

We base the control strategies on the nine composite age-infection states obtained by interacting the latency-defined age categories (*Young*: 0-5; *Mature*: 6-19; *Old*: 20 and above) with the infection categories (E, I_m and I_h). Disease control strategies consist in roguing and replacing infected grapevines that are in one of the three age categories and in one of the three infection categories. They are compared to a baseline case of no control. The infection-age control strategies are then: no disease control (baseline case); roguing and replacing vines that are *Exposed* and *Young* (aged 0-5); *Exposed* and *Mature* (aged 6-19); *Exposed* and *Old* (aged 20 and above); *Infective-moderate* and *Young* (aged 0-5); *Infective-moderate* and *Mature* (aged 6-19); *Infective-moderate* and *Old* (aged 20 and above); *Infective-high* and *Mature* (aged 6-19); and, *Infective-high* and *Old* (aged 20 and above)[12]. We include three additional disease control scenarios that target grapevines in one of the three infection states regardless of age to examine the role of age heterogeneity in GLRD diffusion and control.

[12] We exclude the strategy of roguing and replacing *Infective-high* and *Young* (aged 0-5) because this age-infection combination cannot be reached; it takes a vine more than 5 years to transition up to the *Infective-high* state.

Given that the *Exposed* state is unobservable (i.e., grapevines in that state are symptomless), the disease control scenarios targeting them consist of sampling and testing grapevines for GLRD-causing viruses. This is accomplished with standard diagnosis methods such as biological or enzyme-linked immunosorbent assays. We impose an upper limit of 1%[13] on the proportion of *Exposed* grapevines that are identified using these tests. Such sampling-and-diagnosing methods are currently not commercially used to scout for *Exposed* grapevines, so we do not have cost data for them. Therefore, we use the results to assess the value of technologies developed to detect the virus in *Exposed* vines in commercial vineyards.

2. Bioeconomic outcomes measured and ranking of control strategies

In order to rank disease control strategies, we employ two measures. The first is the expected half-life of the vineyard and the other is the vineyard expected net present value. We define the expected half-life of the vineyard as the expected time period it takes for the total number of healthy vines to decrease by half, that is the time it takes for the disease to reach 50% prevalence. From the ecological part of the model, the desired disease control strategies are those that increase the half-life the most, when compared to the baseline case of no control. On the economic side of the model, among the subset of disease control strategies, the optimal ones are those that yield the highest expected net present value as defined in equation (10). The expected half-life and the expected net present value are obtained from sets of 1,000 simulations for each treatment and the baseline case.

[13] In the current model, this upper limit is selected exogenously. We are implementing a procedure to use the empirical binomial probability density function to describe the probability of detecting *Exposed* vines through sampling.

D. Results and Discussions

In this section we select the strategies that perform better than the baseline in terms of extending the expected vineyard half-life and in terms of maximizing the vineyard expected net present value.

1. Impact of age-infection disease control strategies on disease diffusion

When disease control strategies are not age-structured, the expected vineyard half-life is 8 to 119 months longer than the baseline, depending on whether highly infected or moderately infected vines are targeted, respectively (tables 3 and 4). Age-structuring the strategies by targeting young, mature, or old vines reduces the expected vineyard half-life extension over the baseline in a range of 0.3 to 39 months (tables 3 and 4). This happens because fewer vines are rogued under such age-structured strategies.

[Table 3 here]

[Table 4 here]

When moderately infected young or mature vines are rogued and replaced, the expected improvement over the baseline is 39 or 26 months, respectively. This improvement is statistically significant at the 1% level. The temporal disease diffusion curves in figure 2 explain why targeting young vines (I_mY) achieves higher vineyard half-life than targeting mature vines[14]. Panels a, b and c show the evolution of the number of vines in each of the infection states (H, E, I_m, I_h, I) in the baseline case, I_mY and I_mM control strategies, respectively. Disease control, visible as dips in the red curve and peaks in the green curve in panel b and panel c, occurs more frequently under the I_mY strategy than under the I_mM strategy. In the latter strategy, disease control waits until newly

[14] Figure 2 shows one single realization of the disease diffusion process. Therefore, the realized half-life (read at the intersection of the red and dark green curves) does not correspond to the mean expected half-lives in tables 3 and 4.

infected vines reach the mature age (5 to 20) before implementation. More frequent roguing and replacement is therefore achieved under strategy I_mY. Figure 3 shows a snapshot of GLRD spatial diffusion in a vineyard, 200 months after initial infection. The figure illustrates the higher level of control under I_mY through the more numerous newly rogued and replanted vines (in light green). Also, disease prevalence in the vineyard is visibly lower under this strategy than in the baseline case (panel a) and in the I_mM strategy (panel c).

[Figure 2 here]

[Figure 3 here]

Roguing and replacing moderately infected vines is not as effective in delaying disease diffusion when old vines are targeted. In fact, any strategy consisting of roguing old vines is unsuccessful at extending the vineyard's expected half-life relative to the baseline, regardless of the infection state targeted (tables 3 and 4). Also, strategies targeting heavily infected vines are equally unsuccessful at controlling disease spread (table 4). One exception is the I_hM strategy which achieves a modest improvement of 5 months relative to the baseline, a magnitude that can be considered negligible, although statistically significant at the 1 percent level (table 4). The control frequency argument mentioned earlier and illustrated in figure 2 also explains why targeting heavily-infected old vines is not effective in controlling disease diffusion. Such strategy has the same drawback of waiting longer to control disease diffusion because of the time period (parameter *Inf* in table 2) it takes a vine to transition from state I_m to state I_h. Intuitively, a vineyard manager might be inclined to wait until a productive vine is heavily infected and/or old before roguing and replacing it in order to reap as many benefits as possible. Our results give an estimate of the vineyard half-life loss incurred by such strategies.

The results of control strategies targeting *Exposed* vines are consistent with the previous results in that roguing old vines does not achieve a significant improvement over the baseline and targeting young vines achieves a better outcome than targeting mature vines (table 5). Our results suggest that the expected improvement in vineyard half-life over the baseline is considerable (up to 34 months) and statistically significant even under our assumption that only 1% of *Exposed* vines are identified through sampling and testing. This highlights the importance of controlling *Exposed* grapevines before they become infectious and contribute to GLRD diffusion. Controlling *Young Exposed* vines is critical given that they have the shortest latency period, i.e. they are the fastest to become infectious after they get infected.

[Table 5 here]

2. Cost-effectiveness of age-infection disease control strategies

We use the objective function of expected net present value maximization as described in equation (10) to incorporate cost-effectiveness in ranking the disease control strategies relative to the baseline. Here, we consider only the strategies that extend the expected half-life relative to the baseline of no control. This objective function takes into account the total amount of control achieved under each strategy to reach the half-life extension but also the timing of that control.

Our simulations indicate that the vineyard's expected net present values over a 50-year period are greater than the baseline's in two of the three age-structured disease control strategies targeting moderately infected vines. The I_mY roguing strategy achieves a higher improvement over the baseline than the I_mM does (table 6). This result confirms the insight given by the half-life measure in table 3. Interestingly, simulations of the strategy that targets all age categories yields the lowest expected net present value, in spite of being the best in extending the half-life of the vineyard. This finding highlights the importance of age-structuring the disease control strategies:

by focusing on young, moderately infected vines, less roguing takes place and a better economic outcome is achieved, compared to a non-age structured strategy. Similarly, targeting *Exposed* vines achieves an improvement of 5 percent in the ENPV, which is substantially higher than the ENPV under a strategy that rogues vines of all ages (table 7). The improvement achieved under the *EY* strategy over the next best strategy can be interpreted as the value of scouting for *Exposed* vines through sampling and testing.

[Table 6 here]

[Table 7 here]

The strategy targeting old, highly infected vines (I_hO) have a 1 percent higher ENPV in comparison to the baseline (table 8). Notably, this improvement is despite the very modest improvement of expected half-life extension of the I_hO strategy relative to the I_hM strategy. One explanation is that the total number of vines rogued under the I_hO strategy is almost half what it is under the I_hM strategy, warrantying lower control costs[15] and a higher ENPV.

[Table 8 here]

In figures 4 and 5, we present the probability density functions (PDFs) and cumulative density functions (CDFs) of the expected net present values (ENPV) for a vineyard over a 50-year period. The CDF plots show that a strategy targeting moderately infected and young vines (I_mY) dominates a strategy targeting highly infected old vines (I_hO), which in turn, dominates a strategy roguing moderately infected and mature vines (I_mM).

[Figure 4 here]

[Figure 5 here]

[15] The reason less roguing happens under the I_hO strategy is simply because, over the 50 years, this composite state can be reached only twice, the first time around year 20 and the second time around year 40.

The preliminary simulation results suggest that the alternative disease control strategies yield different results through the timing of disease control that they achieve. A manager deciding when and how often to control GLRD (i.e., what age and infection states to target) faces multiple tradeoffs between the ecological benefits of controlling earlier and the economic costs and benefits of doing so. On the one hand, the more frequent disease control, the more effective in slowing down disease spread and in removing vines as soon as they become symptomatic and infectious. As a result, earlier, more frequent disease control implies lower expected damages. On the other hand, disease control involves two types of costs that incentivize a vineyard manager to postpone roguing depending on her discount rate. Those are labor, machinery and material costs involved in roguing and replacing vines ($c_{i,j}$) and the opportunity cost of roguing and replacing. The latter cost consists of the forgone revenues during the time newly planted vines are still unproductive following replanting (equation 10). However, postponing those costs means incurring two additional types of cost: one is the reduction in revenues of uncontrolled infected vines ($r_{w_{i,j,},t}$) and the other is the expected economic losses that those vines will generate by spreading the infection to uninfected vines.

The results under the parameters considered in this paper show that, for the sub-class of strategies evaluated, it is worthwhile to incur the costs of disease control earlier in order to reap the benefits of a longer vineyard life later. That is, it is better to target younger vines in their earlier infection stages than older vines. Similarly, it is better to target moderately infected vines than heavily infected vines. Those results are affected by a vineyard manager's discount rate: higher values of this rate (lower values of the discount factor ρ), reflecting a more 'economically impatient' manager, would result in postponing disease control, i.e. targeting older vines in more advanced infection stages. The results depend also on the disease control cost and grapevine

revenue parameters (table 3) that we have gathered for New York Cabernet franc vineyards. More expensive disease control, and/or lower grapevine value (lower market price) would also contribute to postponing the disease control decisions, which would favor older age categories and more advanced infection stages.

E. Concluding remarks

We offer a bioeconomic model of disease diffusion and control that addresses some of the limiting assumptions in existing models by allowing agent heterogeneity and fully characterizing the disease spatial-dynamic process. We apply this model to the case of grapevine leafroll disease in a vineyard and evaluate alternative disease control strategies. The simulation results are valuable for vineyard managers as they highlight tradeoffs between the ecological and economic components of complex adaptive systems such as agricultural diseases. Further research should include the formulation and evaluation of a new class of spatial roguing and replacement strategies. The study of spatial control strategies might reveal the potential of alternative vineyard spatial configurations in controlling insect-transmitted viral disease diffusion.

References

Atallah, S.S., M. I. Gómez, M. F. Fuchs, and T. E. Martinson. 2012. Economic Impact of Grapevine Leafroll Disease on *Vitis vinifera* cv. Cabernet franc in Finger Lakes Vineyards of New York. *Am. J. Enol. Vitic*. 63:73-79

Babcock, B. A., E. Lichtenberg, D. Zilberman. 1992. Impact of Damage Control and Quality of Output: Estimating Pest Control Effectiveness. *American Journal of Agricultural Economics* (74), no. 1, 163-172

Bos, L. 1982. Crop losses caused by viruses. *Crop Protection* 1: 263-282

Brauer, F., and C. Castillo-Chavez. 2001. Mathematical Models in Population Biology and Eqidemiology, Texts in Applied Mathematics 40, Springer-Verlag, New York

Cabaleiro, C., C. Couceiro, S. Pereira, M. Barrasa, and A. Segura. 2008. Spatial analysis of epidemics of Grapevine leafroll associated virus-3. *Eur. J. Plant Pathol*. 121:121-130

Cabaleiro, C. and A. Segura. 2006. Temporal analysis of grapevine leafroll associated virus 3 epidemics. European Journal of Plant Pathology 114:441–446

Calonnec, A., P. Cartolaro and J. Chadoeuf. 2009. Highlighting features of spatiotemporal spread of powdery mildew epidemics in the vineyard using statistical modeling on field experimental data. *Phytopathology* 99:411-422

Chan, M-S, and M. J. Jeger. 1994. An Analytical Model of Plant Virus Disease Dynamics with Roguing and Replanting. *J. Appl. Ecol.* 31, no. 3: 413-27

Charles, J., K. Froud, R. van den Brink, and D. Allan. 2009. Mealybugs and the spread of Grapevine leafroll-associated virus 3(GLRaV-3) in a New Zealand Vineyard. *Australasian Plant Pathology* 6:576-83

Charles, J., D. Cohen, J. Walker, S. Forgie, V. Bell and K.Breen. 2006 .A review of the ecology of grapevine leafroll associated virus type 3 (GLRaV-3). *New Zealand Plant Protection* 59:330-337

Epanchin-Niell, R. S. and J.E. Wilen. 2012. Optimal spatial control of biological invasions. *Journal of Environmental Economics and Management* 63: 260-270

Fenichel E. P. and Horan R. D. 2007. Gender-Based Harvesting in Wildlife Disease Management. *American Journal of Agricultural Economics* 89 (4):904-920

Freeborough, M.J., and J. Burger. 2008. Leafroll: Economic implica-tions. [w w w.wynboer.co.za/recentar ticles/200812-leafroll.php3] Wynboer December 2008.

Fuchs, M., P. Marsella-Herrick, G.M. Loeb, T.E. Martinson, and H.C. Hoch. 2009. Diversity of ampeloviruses in mealybug and soft scale vectors and in grapevine hosts from leafroll-affected vineyards. Phytopathology 99:1177-1184.

Gilbert N. 2008. Agent-based model- Quantitative Applications in the Social Sciences. London: SAGE Publications

Gilbert N. and P. Terna. 2000. How to build and use agent-based models in social science. *Mind and Society* 1, no. 1: 57-72

Golino, D.A., E. Weber, S.T. Sim, and A. Rowhani. 2008. Leafroll disease is spreading rapidly in a Napa Valley vineyard. Calif. Agric. 62:156-160.

Goheen, A.C., and J.A. Cook. 1959. Leafroll (red-leaf or rougeau) and its effects on vine growth, fruit quality, and yields. Am. J. Enol. Vitic. 10:4:173-181

Gómez, M., Atallah S., Fuchs M., Martinson T., and White G., 2010. Economic impact of the grape leafroll virus (GLRV) in the Finger Lakes region of New York. Extension Bulleting No. EB-2010-15, Charles H. Dyson School of Applied Economics and Management , Cornell University

Greenhalgh, D. 2011. Age-structured models and optimal control in mathematical epidemiology: a survey. *In* Optimal Control of Age-Structured Populations in Economy, Demography, and the Environment. Routledge Explorations in Environmental Economics. Boucekkine,R, N. Hritonenko and Y. Yatsenko (eds.), Routledge.

Greenhalgh, D. 1986. Control of an Epidemic Spreading in a Heterogeneously Mixing Population. *Mathematical Biosciences* 80:23-45

Harper, F.R., Nelson, G.A. and Pitman, U.J. 1975. Relationship between leaf roll symptoms and yield of Netted Gem potato. *Phytopathology* 65, 1242-1244

Hall, D. C. and Norgaard, R. B. 1973. On the timing and application of pesticides. *American Journal of Agricultural Economics* 55, 198-201

Holt J. and T. C. B. Chacellor. 1996. Simulation Modelling of the Spread of Rice Tungro Virus Disease: The Potential for Management by Roguing. *Journal of Applied Ecology* 33 (5): 927-936

Horan, R. D., E. P. Fenichel, C. A. Wolf, and B. M. Gramig. 2010. Managing infectious animal disease systems. *Annual Review of Resource Economics* 2:101-124

Horan, R.D., and C.A. Wolf. 2005.The Economics of Managing Infectious Wildlife Disease. *American Journal of Agricultural Economics* 87(3): 537–551

Jooste, A. E. C., G. Pietersen and J. T. Burger. 2011. Distribution of grapevine leafroll associated virus-3 variants in South African vineyards. *Eur. J. Plant Pathol.* 131:371 – 381

Macal C. M. and M. J. North. 2010. Tutorial on agent-based modeling and simulation. *J. of Simulation* 4: 151-162

Martelli, G.P., and E. Boudon-Padieu. 2006. Directory of infectious diseases of grapevines. International Centre for Advanced Mediterranean Agronomic Studies. Options Méditerranéennes Ser. B, Studies and Research 55:59-75.

Mar tin, R.R., K.C. East well, A. Wagner, S. Lamprecht, and I.E. Tzanetakis. 2005. Survey for viruses of grapevine in Oregon and Washington. Plant Dis. 89:763-766.

Martinson, T.E., M. Fuchs, G. Loeb, and H.C. Hoch. 2008. Grapevine leafroll: An increasing problem in the Finger Lakes, the US and the world. Finger Lakes Vineyard Notes 6:6-11.

Miller, J. H. and S. E. Page, .2007. Complex Adaptive Systems: An Introduction to Computational Models of Social Life. Princeton University Press

NRAES. 2008. Wine Grape Production Guide for Eastern North America. Natural Resource, Agriculture, and Engineering Service (NRAES) Cooperative Extension

Osgood, N. 2007. Using Traditional and Agent Based Toolsets for System Dynamics: Present Tradeoffs and Future Evolution. *System Dynamics*, 2007.

Pietersen, G. 2006. Spatio-temporal dynamics of grapevine leafroll disease in Western Cape vineyards . Extended Abstracts, 15th Meeting of the International Council for the Study of Virus and Virus-like Diseases of the Grapevine, 2006. Stellenbosch, South Africa, pp 126-127.

Rahmandad H. and J. Sterman. 2008. Heterogeneity and Network Structure in the Dynamics of Diffusion: Comparing Agent-Based and Differential Equation Models. *Management Science*, 54(5):998–1014

Sanchirico, J. and J. Wilen. 2005. Optimal spatial management of renewable resources: matching policy scope to ecosystem scale. *Journal of Environmental Economics and Management* 50: 23–46

Sanchirico, J. and J. Wilen. 1999. Bioeconomics of spatial exploitation in a patchy environment, *Journal of Environmental Economics and Management* 37: 129-150

Saphores, J.D.M. 2000. The economic threshold with a stochastic pest population: a real options approach, *American Journal of Agricultural Economics* 82: 541–555.

Tahvonen, O. 2011. Age-structured optimization models in fisheries bioeconomics: a survey. *In* Optimal Control of Age-Structured Populations in Economy, Demography, and the Environment. Routledge Explorations in Environmental Economics. Boucekkine,R, N. Hritonenko and Y. Yatsenko (eds.), Routledge.

Teose M., K. Ahmadizadeh, E. O'Mahony, R. L. Smith, Z. Lu, S. E. Ellner, C. Gomes, Y. Grohn 2011. Embedding System Dynamics in Agent Based Models for Complex Adaptive Systems. Twenty-Second International Joint Conference on Artificial Intelligence, Barcelona, Spain, July 16-22, 2011

Tesfatsion L., and K. L. Judd (ed.). 2006. Handbook of Computational Economics, Elsevier, edition 1, volume 2, number 2

Tsai, C.W., A. Rowhani, D.A. Golino, K.M. Daane, and R.P.P. Al-meida. 2010. Mealybug transmission of grapevine leafroll viruses: An analysis of virus-vector specificity. *Phytopathology* 100:830-834.

Wilen, J. 2007. Economics of spatial–dynamic processes, *American Journal of Agricultural Economics* 89: 1134–1144.

White, G. 2008.Cost of establishment and production of vinifera grapes in the Finger Lakes region of New York. College of Agriculture and Life Sciences, Cornell University, Ithaca, NY

White R. and G. Engelen. 2000. High-resolution integrated modeling of the spatial dynamics or urban and regional systems. *Computers, Environment and Urban Systems* 24: 383-400.

Tables

Table 1. Modeling potential continuum from traditional to agent-based tools

Equation-based tools	*Agent-Based tools*
Precise	Precise and flexible
Focus on equilibrium states	Inherently dynamic
1, 2, or infinite number of agents	1, 2, …, *N* agents
Non-spatial or partially-spatial	Fully spatial
Homogenous agents	Heterogeneous agents

Adapted from Miller and Page (2007)

Table 2. Model parameters

Parameter	*Description*	*Value*	*Unit*	*Sources*
α	same-row rate of transition from *H* to *E*	4.2*	month $^{-1}$	Values calibrated to yield disease progression curves consistent with those reported in Cabaleiro and Segura (2006); Cabaleiro et al (2008), and Charles et al (2009)
β	adjacent-row rate of transition from *H* to *E*	0.014	month $^{-1}$	
L_y	latency period for young vines (i.e. period spent in *E* before transposing to *I*)	24	months	Discussions with experts based on field observation. Experimentation in progress.
L_m	latency period for mature vines	48	months	
L_o	latency period for old vines	72	months	
Inf	period spent in state I_m before a vine transitions to state I_h	36	months	
τ_{max}	period from planting until productivity	36	months	White (2008)
T_{max} ,A_{max}	maximum model time, maximum vine age	600	months	White (2008)
ρ	discount factor	0.9959	month $^{-1}$	Assumed. Equivalent to an annual discount rate of 5%
$c_{i,j}$	unit cost of vine roguing (removal) and replacement	3.33	\$/vine	Based on White (2008) and Atallah (2012)
$r_{w_{i,j},t}$	revenue of a vine in age-infection state		\$/vine	Vine value based on White (2008) for Cabernet franc
	$A_{i,j} \leq 3$	0		Value reduction based on Atallah (2012) and references therein.
	$A_{i,j} \geq 4$ and *H*	5.12		
	$A_{i,j} \geq 4$ and *E*	3.22		
	$A_{i,j} \geq 4$ and I_m	2.30		
	$A_{i,j} \geq 4$ and I_h	1.15		

* Transmission rates are assumed to be constant for a particular location over the 50 year period of study. This excludes for instance situations where new insect vectors can be introduced and contribute to an increase in the transmission rates.

Table 3. Targeting moderately infected (I_m) vines with and without age-structure: impact on vineyard half-life

Expected half-life [a]	***Mean***	***Expected improvement over baseline*** [b]	
months	*months*	*months*	*percent*
Baseline	203 (10)[c]		
Moderately infected and Young *(I_mY)*	242 (11)	39 ***	19%
Moderately infected and Mature *(I_mM)*	229 (07)	26 ***	13%
Moderately infected and Old (I_mO)	203 (10)	0.27*	0.1%
Moderately infected (I_m), all ages	320 (97)	119***	58%

[a] Expectation are obtained from 1,000 simulations;
[b] Expected half-life improvement = mean (scenario)- mean (baseline); [c] Standard deviations in parentheses;
* Difference in ENPV is significant at the 10% level using estimations with robust standard errors
*** Difference in ENPV is significant at the 1% level using estimations with robust standard errors

Table 4. Targeting highly infected (I_h) vines with and without age-structure: impact on vineyard half-life

Expected half-life [a]	***Mean***	***Expected improvement over baseline*** [b]	
months	*months*	*months*	*percent*
Baseline	203 (10)[c]		
Highly infected and Young *(I_hY)*	n/a	n/a	n/a
Highly infected and Mature *(I_hM)*	208 (10)	5 ***	3%
Highly infected and Old (I_hO)	203 (10)	0.3*	0.1%
Highly infected (I_m), all ages	211 (11)	8***	4%

[a] Expectation are obtained from 1,000 simulations;
[b] Expected half-life improvement = mean (scenario)- mean (baseline); [c] Standard deviations in parentheses;
n/a: not applicable; see footnote 12
* Difference in ENPV is significant at the 10% level using estimations with robust standard errors
*** Difference in ENPV is significant at the 1% level using estimations with robust standard errors

Table 5. Targeting exposed (*E*) vines with and without age-structure: expected gross benefit (months) of uncovering the state of asymptomatic vines

Expected half-life [a]	***Mean***	***Expected improvement over baseline*** [b]	
months	*months*	*months*	*percent*
Baseline	203 (10)[c]		
Exposed and Young *(EY)*	233 (9)	30***	15%
Exposed and Mature (*EM*)	206 (9)	3***	2%
Exposed and Old (*EO*)	203 (10)	0.3*	0.1%
Exposed, all ages (*E*)	237 (9)	34***	17%

[a] Expectation are obtained from 1,000 simulations;
[b] Expected half-life improvement = mean (scenario)- mean (baseline); [c] Standard deviations in parentheses;
* Difference in ENPV is significant at the 10% level using estimations with robust standard errors
*** Difference in ENPV is significant at the 1% level using estimations with robust standard errors

Table 6. Targeting moderately infected (I_m) vines with and without age-structure: impact on vineyard ENPV

ENPV [a]	***Mean***	***Expected improvement over baseline*** [b]	
		million	*percent*
million dollars	*million dollars*	*dollars*	
Baseline	3.796 (0.042)[c]		
Moderately infected and Young *(I_mY)*	3.961 (0.038)	0.166***	4%
Moderately infected and Mature *(I_mM)*	3.819 (0.044)	0.023***	1%
Moderately infected and Old (I_mO)	3.745 (0.045)	-0.051***	-1%
Moderately infected (I_m), all ages	3.620 (0.050)	-0.176***	-5%

[a] Expectation are obtained from 1,000 simulations;
[b] ENPV improvement = mean (scenario)- mean (baseline); [c] Standard deviations in parentheses;
*** Difference in ENPV is significant at the 1% level using estimations with robust standard errors

Table 7. Targeting exposed (E) vines with and without age-structure: expected gross benefit (million dollars) of uncovering the state of asymptomatic vines

ENPV [a]	***Mean***	***Expected improvement over baseline*** [b]	
million dollars	*million dollars*	*million dollars*	*percent*
Baseline	3.796 (0.042)[c]		
Exposed and Young *(EY)*	3.994 (0.041)	0.198***	5%
Exposed and Mature (*EM*)	3.736 (0.045)	-0.060***	-2%
Exposed and Old (*EO*)	3.750 (0.042)	-0.045***	-1%
Exposed, all ages (*E*)	3.444 (0.051)	0.351***	-9%

[a] Expectation are obtained from 1,000 simulations;
[b] ENPV improvement = mean (age-structured scenario)- mean (all ages-scenario); [c] Standard deviations in parentheses;
*** Difference in ENPV is significant at the 1% level using estimations with robust standard errors

Table 8. Targeting highly infected (I_h) vines with and without age-structure: impact on vineyard ENPV

ENPV [a]	***Mean***	***Expected improvement over baseline*** [b]	
million dollars	*million dollars*	*million dollars*	*percent*
Baseline	3.796 (0.042)[c]		
Highly infected and Young *(I_hY)*	n/a	n/a	n/a
Highly infected and Mature *(I_hM)*	3.728 (0.045)	-0.068***	-2%
Highly infected and Old (I_hO)	3. 834 (0.044)	0.037***	1%
Highly infected (I_h), all ages	3. 689 (0.047)	-0.107***	-3%

[a] Expectation are obtained from 1,000 simulations;
[b] ENPV improvement = mean (scenario)- mean (baseline); [c] Standard deviations in parentheses;
n/a: not applicable; see footnote 12
*** Difference in ENPV is significant at the 1% level using estimations with robust standard errors

Figures

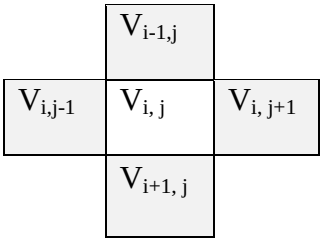

Figure 1. von Neumann neighborhood of vine $V_{i,\ j}$

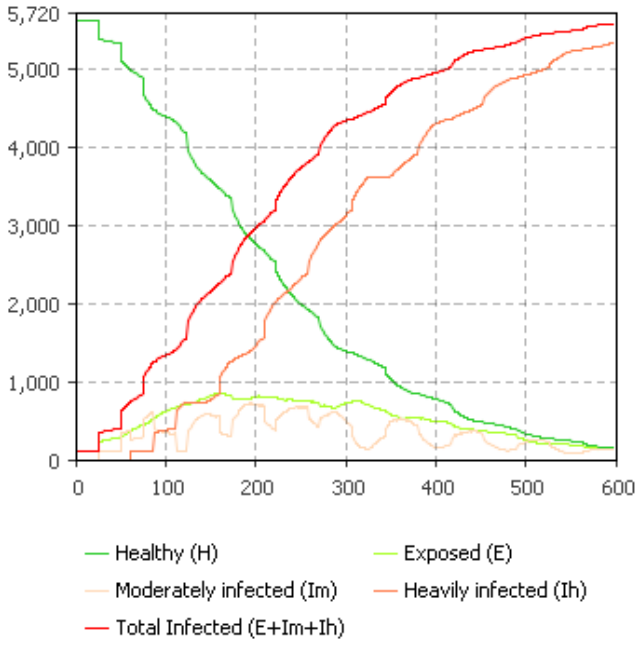

a. Baseline case of no disease control

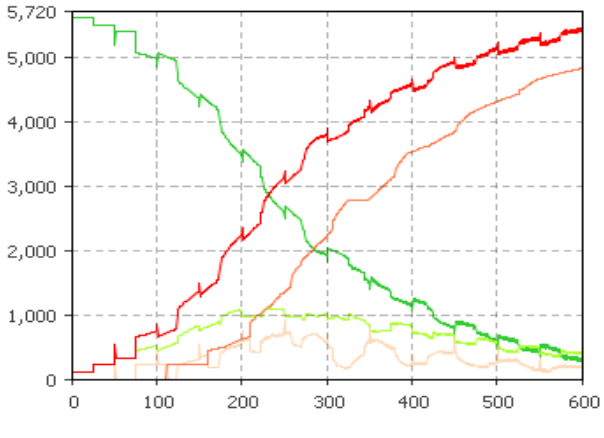

b. I_mY control strategy

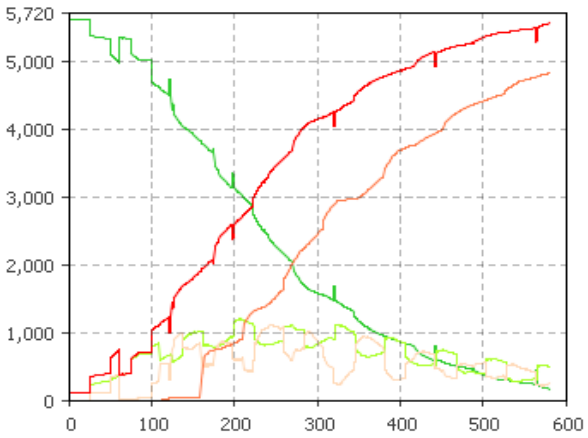

c. I_mM control strategy

Figure 2. Single realizations of temporal disease diffusion for the baseline case of no control (a), and the disease control strategies targeting moderately infected vines that are either young (I_mY) (b) or mature (I_mM) (c). Half-life is read on the x axis (months) at the point of intersection between *Healthy* and *Total Infected*)

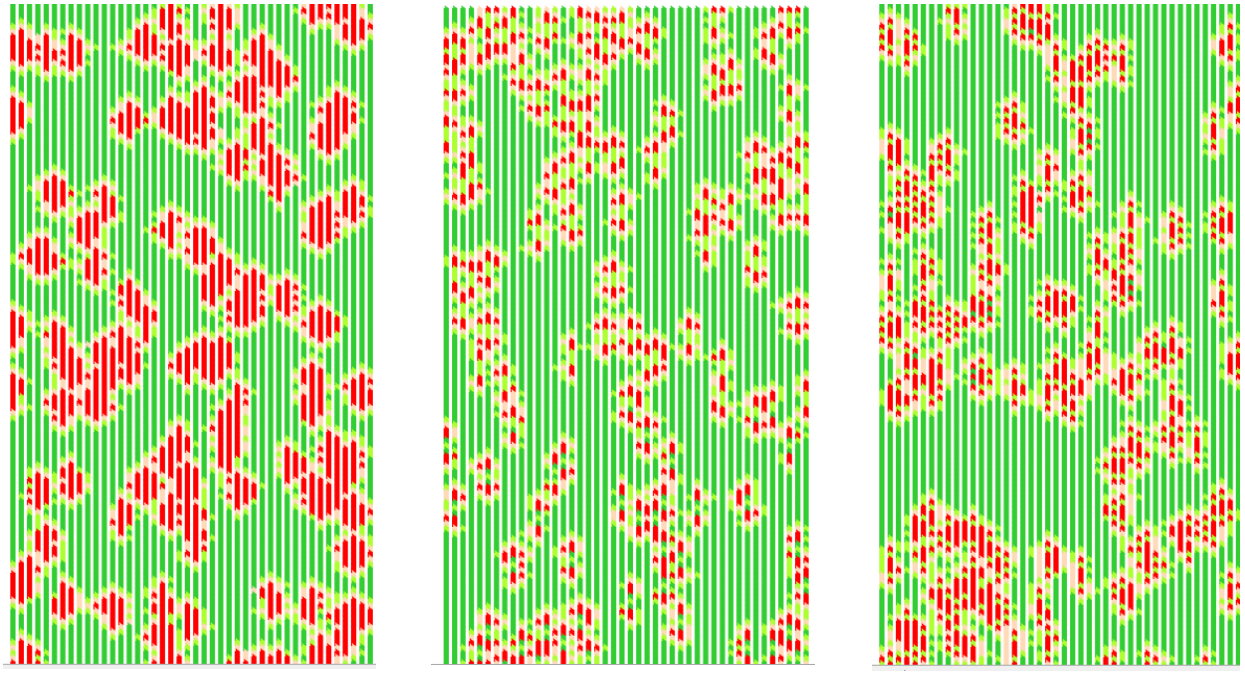

a. Baseline case of no disease control b. I_mY control strategy c. I_mM control strategy

Figure 3. Single realizations of the spatial disease diffusion in a vineyard at t=200 months for the baseline case of no control (a), and the disease control strategies targeting young (I_mY) or (b) or mature (I_mM) moderately infected vines. Color legend is the same as in figure 2.

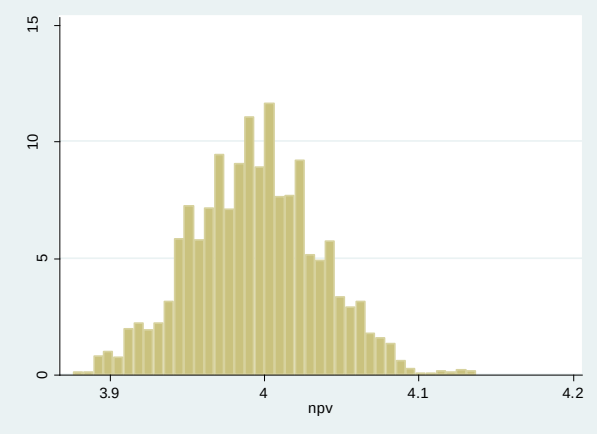

EY PDF

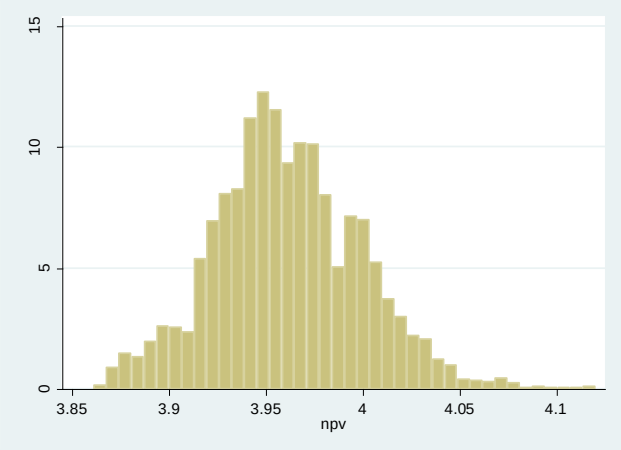

I_mY PDF

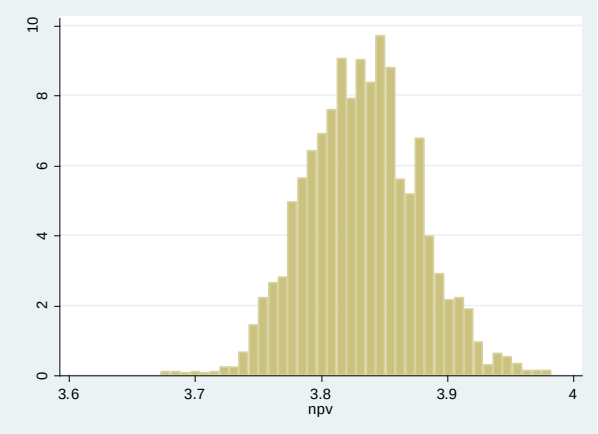

I_hO PDF

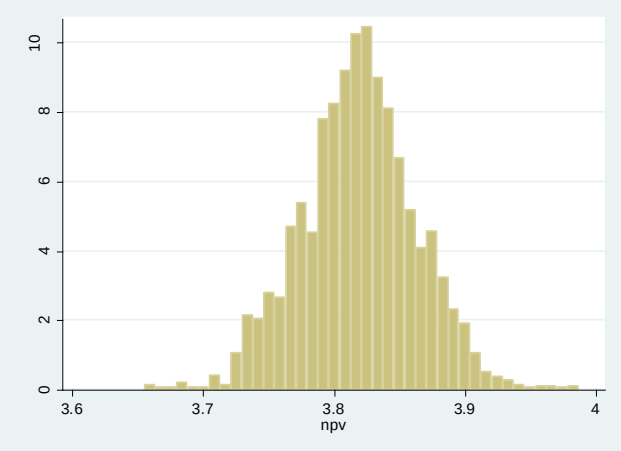

I_mM PDF

Figure 4. PDFs of the ENPV ($) under the *EY*, I_mY , I_hO and I_mM disease control scenarios

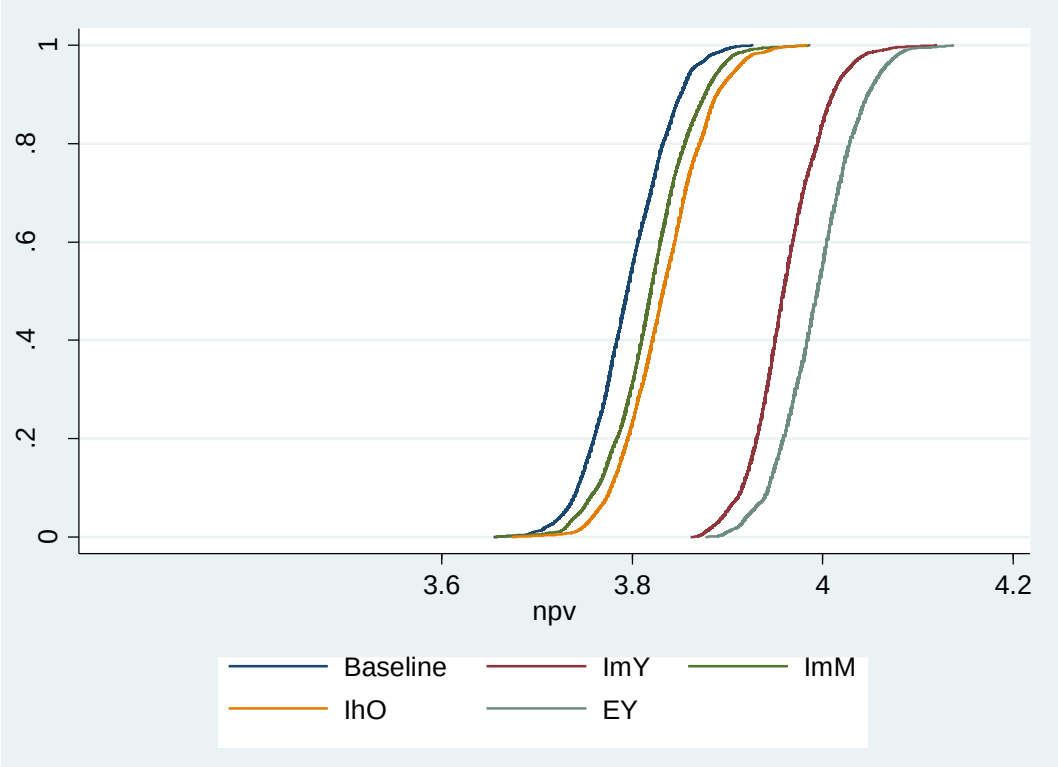

Figure 5. CDFs of the expected vineyard net present value over 50 years for the baseline, *ImY* and *ImM* control strategies